Electronic Supplementary Material (ESI) for CrystEngComm.

Supporting information

New Fourier Transformation Method for SAXS of Polymer Lamellar Crystals

Xiangyang Li*, Jianjun Ding, Pujing Chen, Kang Zheng, Lin Chen and Xingyou Tian

Institute of Applied Technology, CAS Key Laboratory of Photovoltaic and Energy Conservation Materials, Hefei Institutes of Physical Science, Chinese Academy of Sciences, Hefei 230088, China

S1. Small-angle X-ray scatterings obtained during isothermal crystallization of iPP at 130 °C

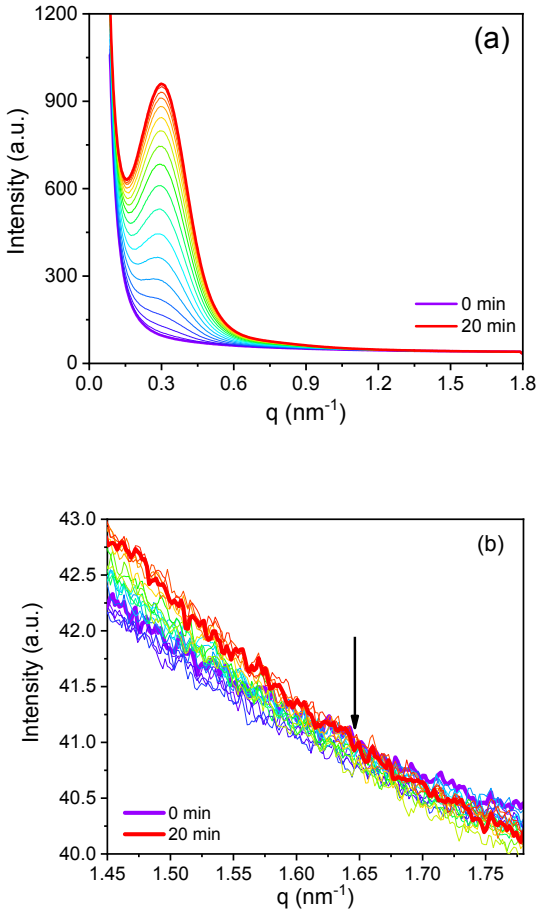

Figure S1. Scattering profiles of iPP collected during isothermal crystallization at 130 °C after removal of thermal history at 220 °C for 5 min.

S2. Determination of form factors of a lamellar crystal and a crystal embryo at

θ_i = 0° and θ_i=15°

Scattering intensity of a crystal plane can be determined with following equation:

$$I_\phi = I_e(\sum_{n=0}^{N-1}\cos n\phi)^2 = (\frac{\sin\frac{N_c\phi}{2}\cos\frac{(N_c+1)\phi}{2}}{\sin\frac{\phi}{2}})^2 I_e \quad \text{(S1)}$$

where N_c is the number of electrons on a crystalline plane, ϕ is the phase difference between adjacent electrons, and I_e is the scattering intensity of a single electron. ϕ is determined with the following equation:

$$\phi = qa\sin(\theta_i\text{-}\theta) \quad \text{(S2)}$$

Here a is the average distance between adjacent electrons, θ_i is the incident angle, θ is the scattered angle. The symbol q is the wave section, which is defined as:

$$q = \frac{4\pi sin\theta}{\lambda} \quad \text{(S3)}$$

The derivation of Eq. 1 and 2 can be seen in our last study (Li et al. IUCrJ 2019, 6, 968–983). Assuming the average distance between adjacent electrons a = 0.17 nm, the number of electrons on a crystal plane with lateral size of l_0 =100 nm is around 588, while the number of electrons on a crystal plane with lateral size of l_0 =10 nm is around 59. Assuming I_e = 1, it can determine the scatterings of the crystal planes with l_0 =10 nm and 100 nm at θ_i = 0° and 15° with N_c and a using Eq. S1-3. The results are shown in Figure 7b-c.